Unsaturated and Transient Seepage Analysis of San Luis Dam

Timothy D. Stark, Ph.D., P.E., D.GE, F.ASCE[1]; Navid H. Jafari, Ph.D., M.ASCE[2]; J. Sebastian Lopez Zhindon, S.M.ASCE[3]; and Ahmed Baghdady, S.M.ASCE[4]

Abstract: This paper uses the San Luis Dam upstream slide to evaluate the pore-water pressures at failure and progression of the phreatic surface through the fine-grained core for drawdown stability analyses. The hydraulic conductivity and compressibility parameters of saturated and unsaturated soils are calibrated using the reservoir hydrograph and 13 piezometers in order to evaluate the pore-water pressures at failure. The analyses show unsaturated and transient seepage analyses can be used to estimate pore-water pressures during drawdown for various stability analyses and evaluate the progression of the phreatic surface through the fine-grained core. The transient results also indicate the van Genuchten parameter α significantly influences unsaturated soil response during drawdown. Different meshing techniques can produce consistent moisture content profiles in two different seepage software packages, but in situ measurement of moisture content and suction pressure is recommended to develop an unsaturated and transient seepage model. **DOI: 10.1061/(ASCE)GT.1943-5606.0001602.**

Author keywords: Rapid drawdown; Transient seepage; Hydraulic conductivity function; Soil water characteristic curve; Unsaturated soil; Compressibility.

Introduction

Sudden or rapid drawdown is typically an important condition controlling the design of the upstream slope in embankment dams and levees (Bishop 1952; Lowe and Karafiath 1959; Bishop and Bjerrum 1960; Morgenstern 1963; Sherard 1953; Sherard et al. 1963; Duncan et al. 1990; Terzaghi et al. 1996; Lane and Griffiths 2000). Numerous reports of slope failure associated with water level fluctuations are reported in Morgenstern (1963), Sherard et al. (1963), and Lane (1967). For example, Jones et al. (1961) investigated landslides that occurred in the vicinity of Roosevelt Lake in the United States from 1941 to 1953. They found about 30% of the slides occurred as a result of reservoir drawdown. The stability of riverbanks under drawdown conditions is also of concern. Desai (1972, 1977) describe experimental and theoretical studies to investigate the stability conditions of Mississippi River earth banks. A report by ICOLD (1980), which reviewed causes of deterioration and failures of embankment dams, determined that a third of the 33 cases of upstream slides were attributed to rapid reservoir drawdown.

[1]Professor of Civil and Environmental Engineering, Univ. of Illinois, Urbana-Champaign 205 N. Mathews Ave., Urbana, IL 61801. E-mail: tstark@illinois.edu

[2]Assistant Professor of Civil and Environmental Engineering, Louisiana State Univ., 3504 Patrick Taylor Hall, Baton Rouge, LA 70803 (corresponding author). E-mail: njafari@lsu.edu

[3]Graduate Research Assistant of Civil and Environmental Engineering, Univ. of Illinois, Urbana-Champaign 205 N. Mathews Ave., Urbana, IL 61801. E-mail: lopezzh2@illinois.edu

[4]Graduate Research Assistant of Civil and Environmental Engineering, Univ. of Illinois, 205 N. Mathews Ave., Urbana, IL 61801. E-mail: baghdad2@illinois.edu

Note. This manuscript was submitted on September 27, 2015; approved on June 22, 2016; published online on August 11, 2016. Discussion period open until January 11, 2017; separate discussions must be submitted for individual papers. This paper is part of the ***Journal of Geotechnical and Geoenvironmental Engineering***, © ASCE, ISSN 1090-0241.

The current state of practice for rapid drawdown analyses involves two approaches: (1) undrained shear stability analyses (USSA), and (2) effective stress stability analyses (ESSA). The USSA method uses undrained shear tests at consolidation pressures prior to drawdown to evaluate shearing resistance (USACE 1970; Lowe and Karafiath 1959; Duncan et al. 1990). ESSA expresses drained shear strength in terms of effective stress parameters and estimates seepage and shear-induced pore-water pressures at drawdown. One advantage of the ESSA method is that drained shear strengths can be determined reliably for use in this method. However, estimating the pore-water pressures is challenging because the dam and subsurface stratigraphy, soil hydraulic conductivity and compressibility properties, and maximum rate of drawdown are necessary to estimate the pore-water pressures during drawdown (Terzaghi et al. 1996).

Existing procedures to estimate pore-water pressures after drawdown include (1) assuming $\bar{B}$, i.e., change in pore-water pressure (Δu) divided by change in the major principal stress ($\Delta\sigma_1$) or ($\Delta u/\Delta\sigma_1$) based on Skempton (1954), is unity for saturated soils (Bishop 1952, 1954; Skempton 1954; Morgenstern 1963; Baker et al. 1993; Lowe and Karafiath 1960; Lane and Griffiths 2000); (2) finite-element unsaturated and transient seepage analyses, which provide pore-water pressure from boundary hydraulic conditions (Desai et al. 1971; Desai 1972, 1977; Wright and Duncan 1987; Stark et al. 2014); and (3) coupled hydro-mechanical finite element analyses (Alonso and Pinyol 2011; Berilgen 2007; Pinyol et al. 2008).

The first procedure ($\bar{B}$) is the sum of transient flow-induced pressure heads and shear-induced pore-water pressure change caused by an instantaneous drawdown (Skempton 1954). In this method, Skempton (1954) defines $\bar{B}$ as

$$\bar{B} = B\left[1 - (1 - A)\left(1 - \frac{\Delta\sigma_3}{\Delta\sigma_1}\right)\right] \quad (1)$$

where the B coefficient = pore-pressures developed from all-around pressures and is about unity (1.0) for saturated soils;

A = shear-induced pore-pressure and is estimated during the application of a deviator stress; and $\Delta\sigma_1$ and $\Delta\sigma_3$ = changes in major and minor principal stresses, respectively. In a triaxial compression test subjected to an isotropic confining stress, increasing the deviator stress generates shear-induced pore-water pressures. Because only shear-induced pore-water pressures are generated in this triaxial compression test, the $\bar{B}$ procedure simplifies to Skempton's A coefficient (Skempton 1954), which can be used to estimate shear-induced pore-water pressures due to reservoir drawdown.

The second procedure predicts transient pore-water pressures using finite-element seepage analyses with transient hydraulic boundaries. This procedure does not include shear-induced pore-water pressures because transient flow is solved using Laplace's equation, which assumes void ratio is constant. Numerical modelling of unsaturated and transient seepage has been investigated by Stark (1987), Lam et al. (1987), Casagli et al. (1999), Rinaldi and Casagli (1999), Pauls et al. (1999), Thieu et al. (2001), Rinaldi et al. (2004), and Berilgen (2007). In particular, Casagli et al. (1999) and Rinaldi et al. (2004) instrumented an eroding bank on the Sieve River in central Italy and validated transient pore-water pressure predictions from seepage analyses for unsaturated soils. In another case study, Pauls et al. (1999) show that predicted pore-water pressures remained well above measured piezometric data for a river bank during a flooding event. This over prediction may be attributed to the uncoupling of stress and flow induced deformations.

The coupled hydro-mechanical analysis best replicates field behavior because it accounts for both shear-induced and transient porous seepage (Alonso and Pinyol 2009). A hydro-mechanical analysis models total head induced flow and volume change induced flow caused by swelling and compression. However, coupled hydro-mechanical models require extensive input parameters and are difficult to use in practice. In contrast, transient seepage analyses are becoming more prevalent to analyze dam and levee seepage and stability performance (Stark et al. 2014).

Lambe and Whitman (1969) define transient flow as the condition during water flow where pore-water pressure, and thus total head, change with time. During transient reservoir conditions, changes in hydraulic boundary conditions cause (1) saturated seepage through relatively pervious foundation strata (Casagrande 1937, 1961; Mansur et al. 1956, 2000; Turnbull and Mansur 1961; Wolff 1974, 1989); and (2) unsaturated seepage through embankment materials (Lam et al. 1987; Cooley 1983). Seepage through saturated soils depends on the hydraulic conductivity in the horizontal direction (k_h), hydraulic conductivity anisotropy ratio (ratio of horizontal k to vertical k or k_h/k_v), and coefficient of volume compressibility (herein referred to as soil compressibility or m_v) of embankment and foundation strata through which seepage will occur (Stark et al. 2014). Unsaturated soil delays seepage and propagation of pore-water pressures in embankments and is controlled by the soil-water retention curve (SWRC) and hydraulic conductivity function (HCF) (Fredlund and Rahardjo 1993). Stark et al. (2014) report the effects of saturated k_h and m_v on saturated foundation strata, but they do not address partially saturated embankment materials.

Because the San Luis Dam material boundaries and rate of drawdown are well-documented (VonThun 1985; Stark 1987; Stark and Duncan 1991) and 13 piezometers were installed after the 1981 upstream slide, the hydraulic conductivity and compressibility properties of saturated and unsaturated soils could be calibrated using a transient seepage analysis. As a result, this study is focused on transient seepage (drawdown and flood loading conditions) through unsaturated embankment soil, e.g., levees and dams, for input in slope stability analyses. In addition, the study investigates the progression of the phreatic surface through the embankment during reservoir operation and the usefulness of unsaturated soil models in two commercial software packages.

Unsaturated and Transient Seepage Theory

The equations for three-dimensional (3D) transient flow (Freeze and Cherry 1979) through a saturated [Eqs. (2*a*) and (2*b*)] and unsaturated [Eq. (2*c*)] anisotropic porous medium are

$$\frac{\partial}{\partial x}\left[k_x\frac{\partial h_t}{\partial x}\right]+\frac{\partial}{\partial y}\left[k_y\frac{\partial h_t}{\partial y}\right]+\frac{\partial}{\partial z}\left[k_z\frac{\partial h_t}{\partial z}\right]=S_s\frac{\partial h_t}{\partial t} \tag{2a}$$

$$\frac{\partial}{\partial x}\left[k_x\frac{\partial h_t}{\partial x}\right]+\frac{\partial}{\partial y}\left[k_y\frac{\partial h_t}{\partial y}\right]+\frac{\partial}{\partial z}\left[k_z\frac{\partial h_t}{\partial z}\right]=\gamma_w m_v\frac{\partial h_t}{\partial t} \tag{2b}$$

$$\frac{\partial}{\partial x}\left[k(h_m)\frac{\partial h_m}{\partial x}\right]+\frac{\partial}{\partial y}\left[k(h_m)\frac{\partial h_m}{\partial y}\right]+\frac{\partial}{\partial z}\left[k(h_m)\left(\frac{\partial h_m}{\partial z}+1\right)\right]=C(h_m)\frac{\partial h_m}{\partial t} \tag{2c}$$

where k = hydraulic conductivity in the x, y, and z directions, h_t = total hydraulic head; and t = time; and S_s = specific storage. Specific storage is expressed as $S_s=\gamma_w(m_v+n\beta)$, where γ_w = unit weight of water; n = porosity; and β = compressibility of water. Because water is incompressible (4.7×10^{-7} kPa^{-1} for seepage purposes, specific storage reduces to $S_s=\gamma_w m_v$ and transforms Eq. (2*a*) into Eq. (2*b*) in seepage software (Stark et al. 2014). In Eq. (2*c*), $k(h_m)$ = hydraulic conductivity function (HCF); $C(h_m)$ = slope of the soil-water retention curve or SWRC; and h_m = matric suction head. Because the time-variant nature of seepage problems is dependent upon movement of the phreatic surface in embankments, applying reasonable unsaturated soil properties is important to accurately model pore-water pressure dissipation during reservoir drawdown. The transient flow in Eq. (2*b*) is solved using Laplace's equation, hence void ratio of the porous soil remains constant and the selected m_v value represents the void ratio at the in situ effective vertical stress. Stark et al. (2014) provide methods to evaluate m_v because this term can significantly affect the time-dependent response of pore-water pressure for saturated soil. As the soil transitions to an unsaturated state in Eq. (2*c*), the time-dependent response of the volumetric water content is now controlled by the SWRC.

The unsaturated properties in an earth embankment influence the flow, stresses, and deformations during reservoir operation or floods. The hydraulic properties are evaluated using a SWRC, which provides a relationship between matric suction and volumetric water content, and is important for predicting the HCF. The SWRC is hysteretic and laboratory experimental techniques usually measure the drying (reservoir lowering) not wetting (reservoir filling) paths. Because of the lack of wetting data, a closed-form function is used to match drying experiments to model unsaturated soils (Lu et al. 2004). The Brooks and Corey (1964), van Genuchten (1980), and Fredlund and Xing (1994) are SWRC models commonly used in geotechnical applications. The van Genuchten (1980) model is a smooth, closed-form model that accounts for the inflection point, is capable of capturing the sigmoidal shape of the SWRC, and matches experimental data more accurately (Valiantzas 2011). Specifically, the van Genuchten (1980) model includes an inflection point which produces the sigmoidal S shape, which is applicable to a wide range of soil types (Stankovich et al. 1995). For example, Bareither and Benson (2013) found van Genuchten (1980) parameters are applicable to bulk soil mainly consistent of gravel, i.e., comparable to coarse grained filter material commonly

used in embankment dams. Additionally, Benson et al. (2014) report van Genuchten (1980) parameters to model clean sands. Tinjum et al. (1997) correlate van Genuchten (1980) parameters to compaction water content, compactive effort, and plasticity index for compacted clays. Because a wide range of materials can be modeled using the van Genuchten (1980) relationship, the San Luis Dam unsaturated soils are characterized using this model.

The van Genuchten (1980) model relates matric suction head (h_m; m) and volumetric water content (θ; cm^3/cm^3) via curve fitting parameters α and n, and m

$$\theta = \theta_r + \frac{\theta_s - \theta_r}{[1 + (\alpha h_m)^n]^m} \tag{3}$$

where θ_s = saturated volumetric water content; θ_r = residual volumetric water content; and $m = 1 - 1/n$. The parameter α is related to the air entry suction head (m^{-1}) and can be converted to the height of the capillary fringe (m) by the reciprocal. The value n corresponds to the soil pore size distribution. The van Genuchten (1980) model determines the HCF by combining the work of Burdine (1953) and Mualem (1976) as shown below:

$$k(h_m) = k_s \sqrt{S_e}[1 - (1 - S_e^{1/m})^m]^2 \tag{4}$$

$$S_e = [1 + (ah_m)^n]^{-m} \tag{5}$$

where $k(h_m)$ = unsaturated hydraulic conductivity; k_s = saturated hydraulic conductivity; and S_e = effective saturation. Fig. 1 shows the sensitivity of α and n for SWRC and HCF for the fine-grained core of San Luis Dam. Assuming $n = 4.5$ in Figs. 1(a and b), increasing α from 0.05 to 2 m^{-1} shifts the SWRC and HCF to lower matric suction because the air entry values (AEV) are decreasing. The AEV and α value are inversely related ($\alpha = 1/\text{AEV}$), e.g., α value of 0.05 m^{-1} yields an air entry suction of 20 kPa and corresponds to a capillary fringe of ~2 m. Because AEV also corresponds to the stage where the largest pores begin to drain and air enters the soil matrix, decreasing AEV permits the desaturation process to initiate sooner. Assuming constant α in Fig. 1(c), increasing the parameter n steepens the SWRC slope between θ_r and θ_s. Thus, increasing n from 1.5 to 6.5 in Fig. 1(d) also steepens the transition from saturated k_h. In summary, Fig. 1 shows that α produces a greater impact on the HCF and SWRC curves than n,

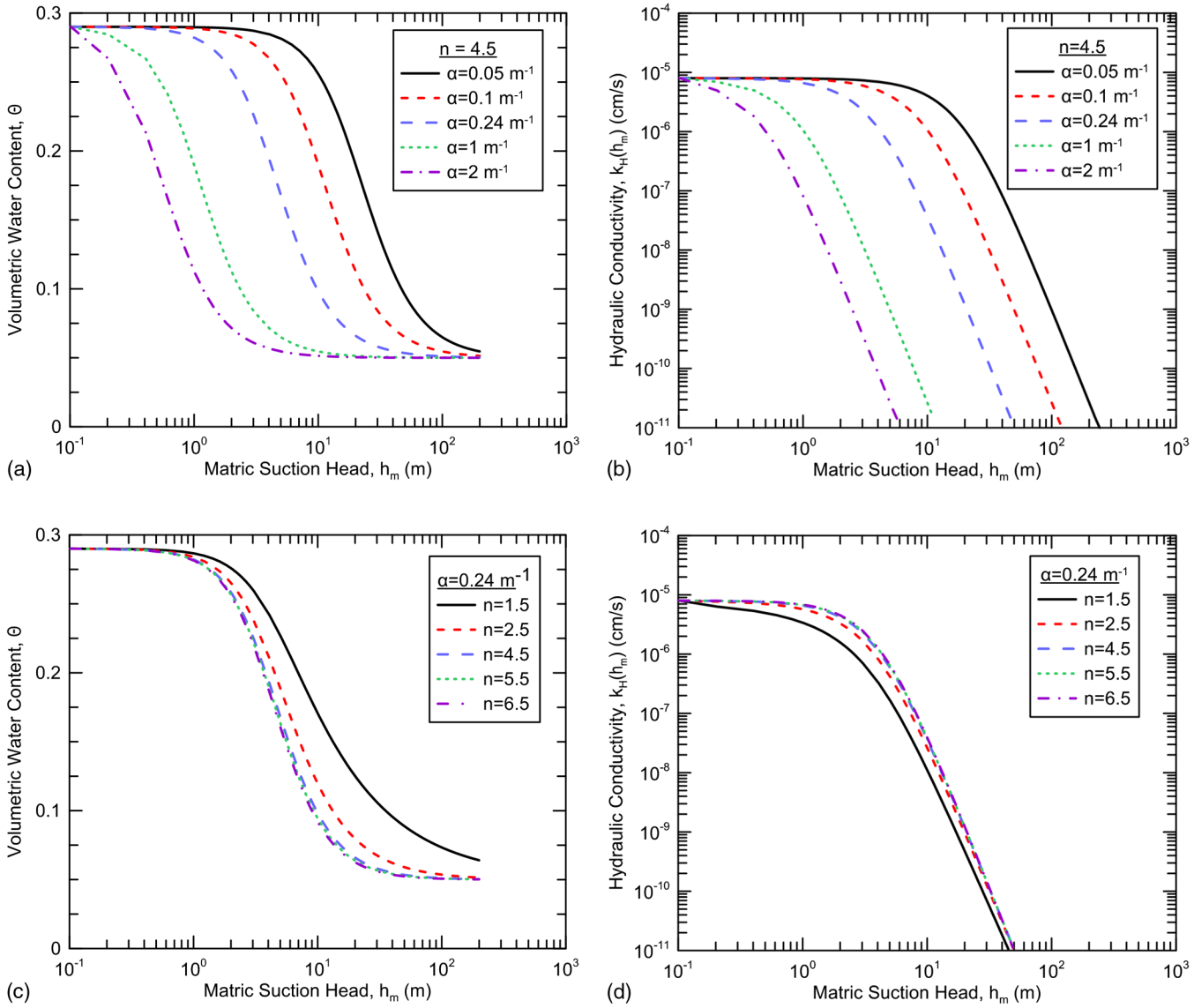

Fig. 1. Zone 1 unsaturated soil properties modeled with van Genuchten (1980) model: (a) SWRC ($n = 4.5$, $\alpha = 0.05$–2); (b) HCF ($n = 4.5$, $\alpha = 0.05$–2); (c) SWRC ($\alpha = 0.24$, $n = 1.5$–6.5); (d) HCF ($\alpha = 0.24$, $n = 1.5$–6.5)

which is negligible for $n \geq 4.5$. This observation is important and reduced the computing time required to calibrate the SWRC and HCF for the fine-grained core.

San Luis Dam

The drawdown case history involves the 1981 upstream slide in San Luis Dam (now known as B.F. Sisk Dam) in California, which is described in VonThun (1985) and Stark and Duncan (1991). Sanctioned in 1960 under the Central Valley Project and the State of California Water Plan, San Luis Reservoir is the largest offstream manmade lake in the United States with a capacity of about 252 million m^3 (USBR 2013). San Luis Reservoir is located approximately 170 km southeast of San Francisco and began filling in 1968. In September 1981, after the reservoir was drawn down 55 m (180 ft) in 120 days, a major slide occurred in the upstream slope (VonThun 1985; Stark and Duncan 1991). Prior to the 1981 slide, San Luis Dam experienced several drawdown cycles, but the 1981 drawdown was the longest and fastest in San Luis Dam history. The slide was about 550 m (1,800 ft) along the centerline of the dam crest.

Failure causation analyses by VonThun (1985) and Stark (1987) found the slide was deep-seated, with the majority of the failure surface located in the slopewash left in the foundation during construction. The construction specifications required the existing hill to be stripped to a horizon that exceeded the strength of the overlying embankment material. Because the slopewash was highly desiccated at the time of construction, it was not removed (Stark and Duncan 1991). Upon reservoir filling and wetting of the desiccated slopewash (see location in Fig. 2), the shear strength reduced to fully softened strength. Then, the possible colluvium nature of the slopewash and cyclic loading from the reservoir water level resulted in shear deformations sufficient to mobilize shear strengths between fully softened and residual values. As a result, the significant reduction in slopewash strength resulted in the slope failure (Stark 1987; Stark and Duncan 1991).

Geology

A geologic cross section of San Luis Dam at Station 135 + 00 is shown in Fig. 2. The bedrock consists of interbedded and faulted sandstone, shale, and conglomerate. In particular, the Gonzaga Fault System dissects the bedrock near the toe of the slope and trends N 50°W and dips 80 to 90°. The slopewash blankets the bedrock in the lower portion of the upstream slope, covering an area that extends from the toe of the dam to a horizontal distance of −60 m in Fig. 2. The slopewash liquid limit (LL), plasticity index (PI), and natural water content (w_o) are about 38–45%, 19–21%, and 7–8%, respectively. The impervious fine-grained core (Zone 1) is a high plasticity clay compacted to +2% wet of optimum and a dry unit weight of 14.5 kN/m^3. The miscellaneous clayey gravel fill (Zone 3) overlying the slopewash is borrow material that originates from the channel excavation and is predominantly clay with LL, PI, and w_o of 28–35%, 14–21%, and 14%, respectively. Zones 4 and 5 are rockfill material buttressing the fine-grained core. Zone 4 consists of minus 20 cm rockfill, while Zone 5 rockfill is plus 20 cm. After the 1981 slide, a stabilizing rockfill berm was constructed at the toe of the slope (Zone 7 in Fig. 2). Table 1 summarizes the soil index properties for the fine-grained soils in Fig. 2. The initial degree of saturation and volumetric water content reported in Table 1 were used in developing the unsaturated soil properties.

Reservoir Hydrograph and Piezometer Locations

Fig. 3 shows the San Luis Reservoir hydrograph from 1968 to 1987. The first filling occurred in 1968 at an approximate rate of 0.11 m/day until the reservoir reached a capacity of Elev. +165 m. The reservoir was maintained at or near Elev. +165 m until 1974 (~6 years), which allowed Zone 3 and slopewash to saturate and approach steady-state conditions in parts of Zone 1 (Stark 1987). After 1974, the reservoir level cycled each year with the lowest level of Elev. +105 m occurring during the 1977 drought (Stark 1987). The drawdown rate of 0.45 m/day that preceded the 1981 slide was the largest and fastest the reservoir had experienced. After

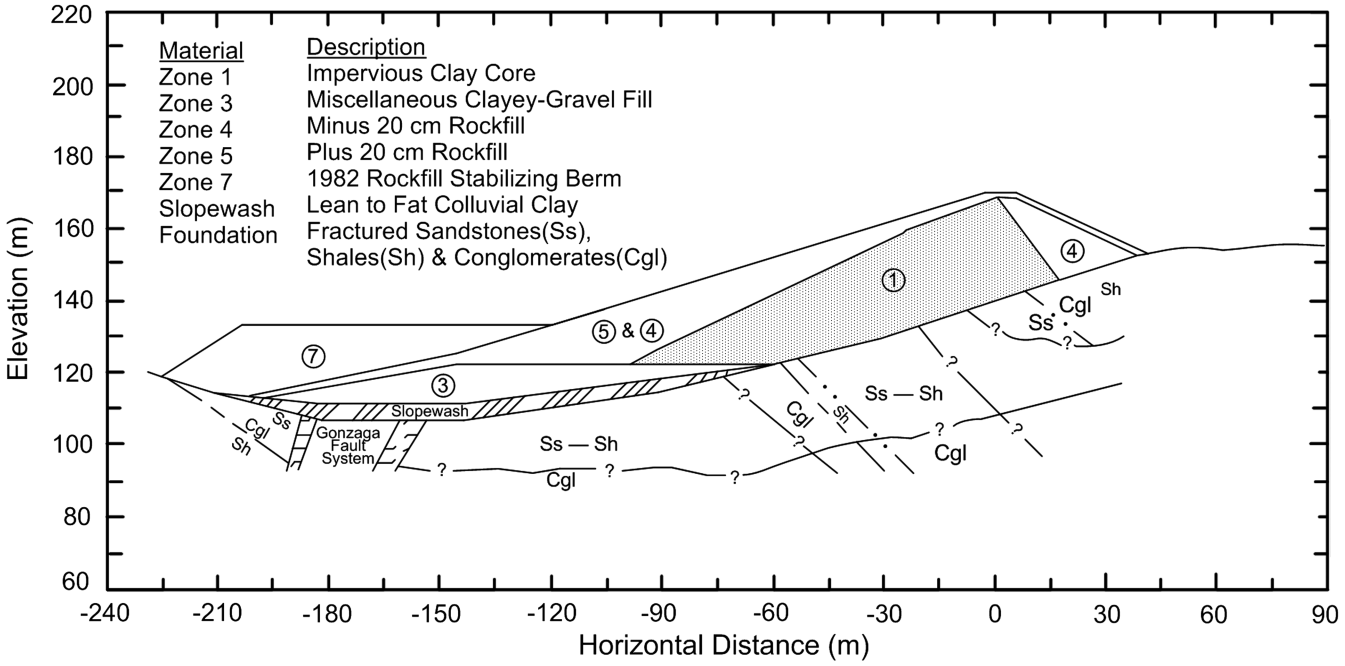

Fig. 2. Geologic cross section of San Luis Dam (adapted from Stark 1987, with permission)

Table 1. Summary of Index and Hydraulic Engineering Properties (Data from Stark 1987)

Soil property	Zone 1	Zone 3	Slopewash
Liquid limit, LL (%)	40–47	28–35	38–45
Plasticity index, PI (%)	23–30	14–21	19–21
Natural water content, w_o (%)	15	14	7–8
Initial degree of saturation, S_r (%)	90	80–85	55–60
Porosity, n	0.29	0.33	0.29
Volumetric water content, θ	0.26	0.26–0.28	0.16–0.17

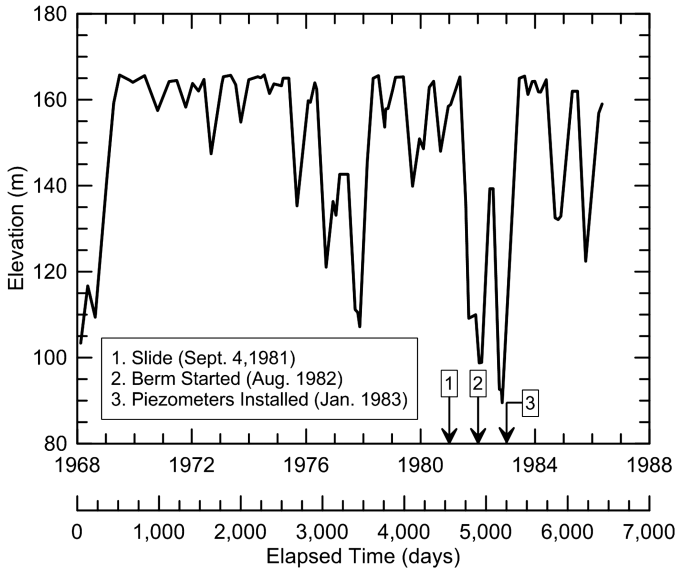

Fig. 3. San Luis Reservoir hydrograph with (1) 1981 upstream slide; (2) berm construction started and was completed in 1983; (3) piezometers installed

the 1981 slide, the reservoir was raised to Elev. +140 m at a rate of 0.10 m/day but was lowered again at a rate of 0.42 m/day to Elev. +90 m in late 1982 for repair. In 1983, the reservoir level was raised to Elev. +165 m at a rate of 0.27 m/day. From 1984 until 1987, the reservoir remained at capacity (lowest level at Elev. +122 m) with two drawdown cycles. The timeline in Fig. 3 indicates the toe berm was started in August of 1982. The piezometers were installed in January 2013, which are used to calibrate the soil seepage properties.

After the stabilizing toe berm was completed in 1983, a total of 13 multilevel piezometers were installed in 5 borings (Fig. 4) to monitor pore-water pressures. Three of the piezometers are located middepth of the slopewash, three in Zone 3, and two in the Zone 1 fine-grained core. The pore-water pressures measured using the piezometers are used to establish the initial seepage boundary conditions for analysis and adjust the seepage parameters to achieve the best agreement between the measured and calculated pressure heads.

Seepage Model

Stark (1987) performed an unsaturated and transient seepage analysis to estimate the seepage induced pore-water pressures within the slopewash and Zone 1 materials for various stability analyses. The material properties reported in Stark (1987) were calibrated using the 1D software *UNSAT-1* (Neumann 1973). In this study, 2D *SEEP/W* and *SLIDE 6.0* finite-element software are used to calibrate soil properties and evaluate pore-water pressures in the slopewash and Zone 1 at the time of failure. *SEEP/W* is a general seepage analysis program formulated to model saturated and unsaturated soils for transient flow and excess pore-water pressure dissipation estimated from a stress-deformation analysis within porous materials. *SLIDE* is a limit equilibrium slope stability software package with built-in finite-element groundwater seepage capabilities for steady-state or transient flow conditions.

SEEP/W and *SLIDE* model unsaturated soils using the SWRC to compare predicted pore-water pressures to the piezometers. While both programs use similar parameters (SWRC and changes in volumetric water contents) and computational methods, the input methods differ when incorporating initial conditions or parent analyses into staged analyses. For example, *SEEP/W* includes the option to link limit equilibrium and/or stress-deformation analyses within the same file. In contrast, *SLIDE* requires a separate file to input the pore-water pressure, total head, or pressure head grid from prior analyses to represent the initial groundwater condition and phreatic

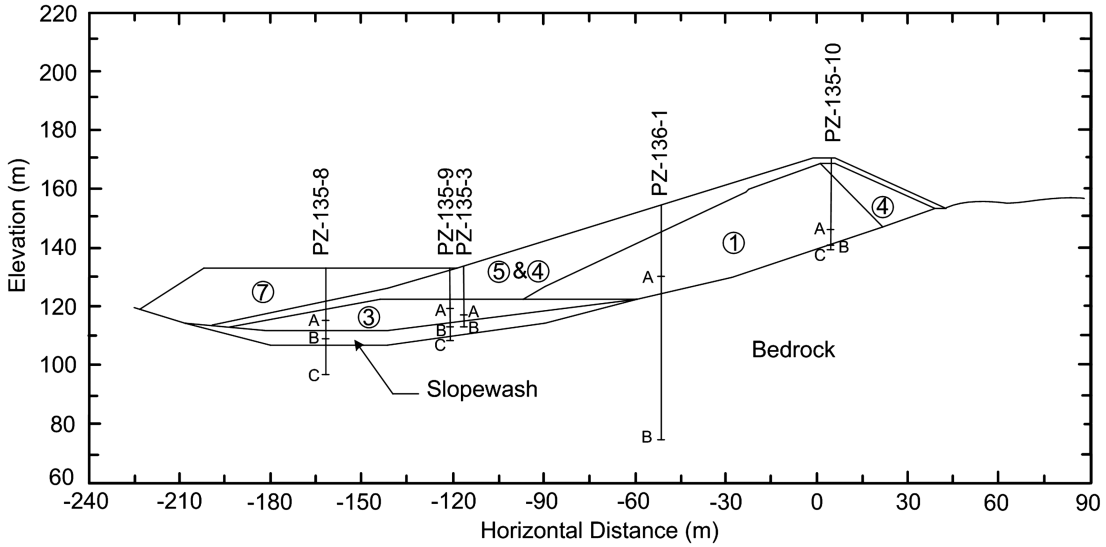

Fig. 4. Location of piezometers installed after the 1981 slide

surface. Meshing options also vary between the two programs. *SEEP/W* uses four-noded quadrilaterals as the sole option for meshing, whereas *SLIDE* offers three, four, six, and eight-node meshing. *SEEP/W* also allows the user to indicate the spacing of the meshing to make a custom mesh. *SLIDE* enables the user to custom discretize or increase the density of mesh, but not to a specified number. The input of unsaturated properties also varies between the two programs. *SEEP/W* and *SLIDE* offer the options to input custom SWRC and HCF from laboratory data or use closed-form models, such as Brooks and Corey (1964) or van Genuchten (1980). For the closed-form models, *SEEP/W* enables the user to define the number of data points used for the SWRC and HCF graphs. Increasing the number of data points allows the software to better capture SWRC curvature and thus model the unsaturated properties more accurately than using a limited number of points. *SLIDE* uses a predefined number of 50 data points to define the SWRC and HCF. To increase the number of data points, the user should use the original closed-form model equation with small matric suction steps, e.g., $\Delta\psi \sim 0.1$ kPa, to compute the SWRC and HCF. The resulting SWRC and HCF can be inserted into *SLIDE* as a custom function. These differences were all accounted for in the case study to produce similar models and results between the two programs.

Parent Analysis

The initial groundwater conditions are used as the origin for the transient seepage analysis. Stark et al. (2014) use a steady-state seepage analysis to develop pore-water conditions for a floodwall case study involving foundation underseepage. In the present study, a steady-state analysis is also used to predict initial matric suction values (prior to reservoir filling) for the San Luis Dam cross section in Figs. 2 and 4. The steady-state analysis is performed in *SEEP/W* and *SLIDE* to compare the predicted phreatic surface and initial matric suctions in the Zone 1, Zone 3, and slopewash materials. For the steady-state analysis, the lefthand side (LHS) and upstream slope boundary conditions are assigned a total head of Elev. +90.6 m, which reflects no reservoir. The righthand side (RHS) total head boundary is set to a total head of 132 m to ensure the slopewash remains unsaturated before reservoir operation begins. The bottom boundary is set to a no flow condition because competent bedrock underlies the dam and slopewash. Fig. 5 superimposes the initial suction contours from *SEEP/W* and *SLIDE*. Both programs predict a matric suction of −600 kPa at the top of Zone 1 fine-grained core and horizontal contour lines in Zones 4 and 5. While there are similarities in the initial suction profile for both programs, there are slight variations in the shape of the contour lines. Fig. 5 shows that *SEEP/W* and *SLIDE* produce similar results throughout the foundation. However, at the downstream slope and throughout Zone 1, the shape of the contours, specifically between −200 to −600 kPa, diverge. The *SLIDE* contours exhibit more curvature in Zone 1 fine-grained core than the *SEEP/W* contours. As both models utilize the same geometries and material properties, the different interpolations of the contours are likely caused by applying a three-node mesh (*SLIDE*) as opposed to a four-node mesh (*SEEP/W*). An additional analysis using the same meshing in both programs produced agreement in the contours. Therefore in seepage analyses using multiple programs, the use of consistent meshing and elements with similar geometries and material properties is necessary to produce similar initial conditions and perform meaningful comparisons.

Transient Boundary Conditions

For a transient seepage analysis, it is essential to define the initial groundwater and boundary conditions. The measured pore-water pressures from January 1983 to March 1986 provide a basis for establishing the seepage boundary conditions and refining the material properties for the transient seepage analyses. The boundary conditions applied in *SEEP/W* and *SLIDE* are shown in Fig. 6. The foundation piezometers (135-9C, 135-8C, and 136-1B) in Fig. 2 show immediate response to reservoir changes, which indicates a hydraulic connection between the foundation and reservoir. The bottom boundary condition is modeled as a no-flow boundary via the no unit flux condition in *SEEP/W* and a zero normal infiltration rate in *SLIDE* to reflect competent bedrock. The reservoir hydrograph in Fig. 3 is applied to the upstream slope and is modeled as a total head boundary in *SEEP/W* and *SLIDE*. The transient analysis is divided into two stages because a toe berm constructed as a remedial measure changes the model geometry. The first stage extends from 1967 to 1983 (0 to 5,665 days) and the second stage from 1983 to 1987 (5,665 to 6,615 days). Readings at piezometer 135-10A in Zone 1 (Fig. 4) remained zero indicating the soil remained unsaturated from 1983 to 1987. In addition, the assumed water surface in the downstream side of the dam corresponds to a pressure head of -15 m. This boundary condition was determined based on field observations of the reservoir tail water and desiccated landside slope of the existing hill. Stark (1987) also indicates the slopewash was desiccated and downstream slope remained unsaturated, so the RHS boundary is modeled with a constant head of 132 m.

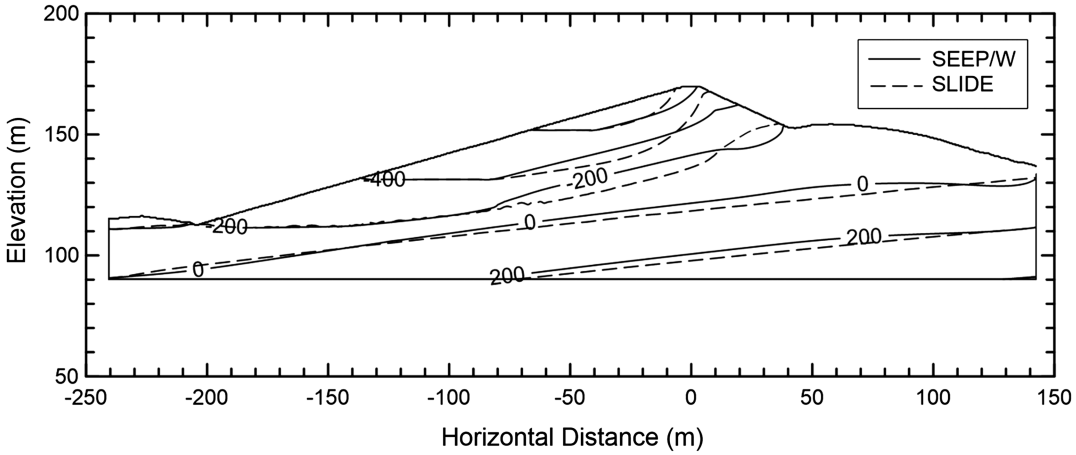

Fig. 5. Comparison of initial suction contours computed with *SEEP/W* and *SLIDE*

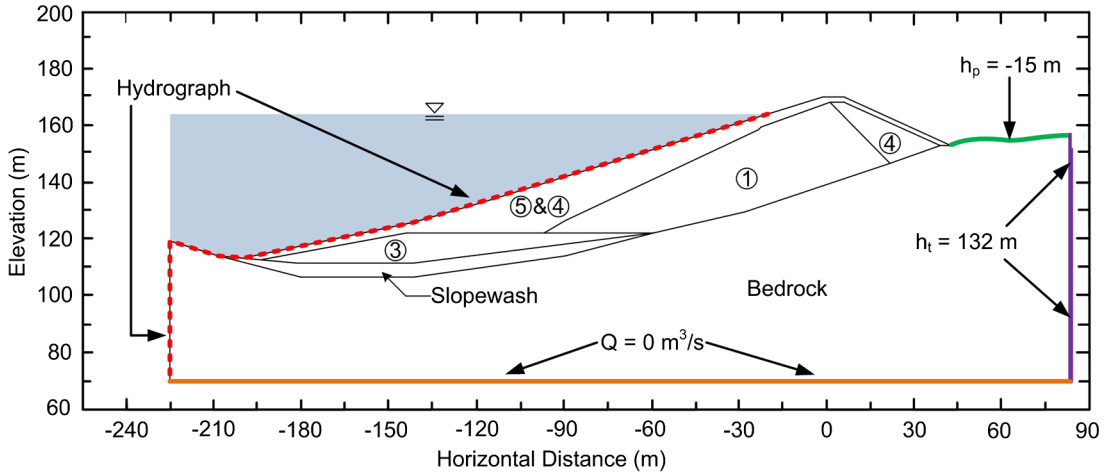

Fig. 6. Boundary conditions applied for transient seepage model

Calibrated Soil Properties

In an unsaturated and transient seepage analysis, four soil properties are required: (1) initial matric suction profile, (2) unsaturated soil properties (SWRC and HCF), (3) saturated k_h/k_v ratio, and (4) soil compressibility (m_v). Soil engineering properties presented in Table 2 are based on laboratory and site data from Stark (1987) and were used as a starting point for model calibration. Unsaturated soil properties are important for Zone 1 because the fine-grained core does not become fully saturated until after the piezometers are installed. The van Genuchten (1980) model SWRC and HCF are applied to the slopewash, Zone 1, and Zone 3 materials. The model calibration of Zone 1 involves varying the van Genuchten (1980) curve fitting parameters α and n while the saturated k_h, k_h/k_v, and m_v are varied for the saturated slopewash and Zone 3. The final soil properties are calibrated using 13 piezometer readings from 1983 to 1986 (elapsed time of 5,665 to 6,665 days). The *SEEP/W* and *SLIDE* models incorporate the steady-state analysis as the initial groundwater conditions (Fig. 5 or "Parent Analysis" section). In addition, the transient analysis is divided into two stages to accommodate the toe berm construction and change in upstream geometry. For *SEEP/W* and *SLIDE*, the model time step is seven days during the 1981 drawdown (4,850 to 5,850 days) and the period of piezometer data (5,665 to 6,615 days) to ensure fluctuations in reservoir levels are accurately captured. All other reservoir operation periods, e.g., constant reservoir levels, used an increased time stepping of 90 days to reduce computation time while also maintaining model accuracy. The meshing in both programs utilized a four-node element with over 5,000 elements to provide accuracy and consistency between the two seepage models.

The transient model is calibrated using piezometers located in the slopewash (PZ-135-8B, PZ-135-9B, PZ-135-3B), Zone 3 (PZ-135-8A, PZ-135-9A, PZ-135-3A), and Zone 1 (PZ-136-1A and PZ-135-10A). Fig. 2 shows that the foundation consists of non-homogenous materials, including fractured sandstones, shales, conglomerates, and the Gonzaga Fault System. Due to uncertainty in spacing and orientation of these fractures, it is difficult to apply these materials in *SEEP/W* and *SLIDE*. Because the bedrock did not play a significant role in the 1981 slide and some uncertainty persists in the bedrock properties, less emphasis is placed on calibrating the response of the foundation piezometers (PZ-135-8C, PZ-135-9C, PZ-136-1B, PZ-135-10B, and PZ-135-10C). Therefore, the calibrated bedrock properties are selected so the response of the slopewash and Zone 1 match the piezometer measurements.

Table 2. Initial Seepage Properties (Data from Stark 1987)

Material	k_h (cm/s)	k_h/k_v	m_v (kPa^{-1})	θ_S	θ_R	$1/\alpha$ (m)	n
Zone 1	2.7×10^{-7}	4	8.4×10^{-6}	0.29	0.05	20	1.3
Zone 3	1.4×10^{-6}	4	3.3×10^{-6}	0.27	0.02	28.6	3.2
Slopewash	4.2×10^{-8}	4	2.3×10^{-5}	0.24	0.02	50	2.6
Foundation	3.8×10^{-6}	4	1.7×10^{-5}	—	—	—	—

The initial seepage analysis shows the Zone 3 and slopewash materials saturate rapidly during the first filling of San Luis Reservoir. Therefore, the saturated k_h, k_h/k_v, and m_v define the total head response of these materials (Stark et al. 2014) and are adjusted to reach agreement between the model and field piezometers measurements. Varying m_v values produces a time lag effect, i.e., pore-water pressure response is accelerated or delayed. For example, Fig. 7 shows plots of total head versus elapsed time. Changes in m_v manifest in Fig. 7 by shifting or translating the total head data, and values of saturated k_h and k_h/k_v affect the total head magnitude, e.g., an increase in either parameter increases the pore-water pressure in the material. The calibration process is not solely focused on the individual response of the slopewash material because interaction of soils layers is present, specifically the foundation bedrock. By lowering the foundation k_h to an impervious material, drainage into the foundation is limited, causing pore-water pressures to build up in the slopewash. In contrast, modeling the foundation as a pervious material allows drainage and decreases the pore-water pressure response in the slopewash.

Preliminary seepage analyses demonstrated that saturated flow from Zone 3 and foundation bedrock influenced the modeled response in the slopewash while the Zone 1 results were influenced by movement of the phreatic surface, i.e., cycles of wetting and drying. Because saturated soil parameters governed the slopewash response and Zone 1 response is a function of unsaturated properties, these soil layers could be calibrated separately. In other words, Zone 1 unsaturated soil parameters were varied until the pore-water pressures were in agreement with field piezometer readings. The slopewash properties were determined by first calibrating Zone 3 followed by the slopewash. The bedrock properties were adjusted at the end of the process to further improve the agreement between modeled and measured slopewash pore-water pressures.

Fig. 7(a) shows the final calibration of the slopewash using PZ-135-9B. The calibration process decreased the saturated k_h by a factor of five (5) from the original value of Stark (1987) and

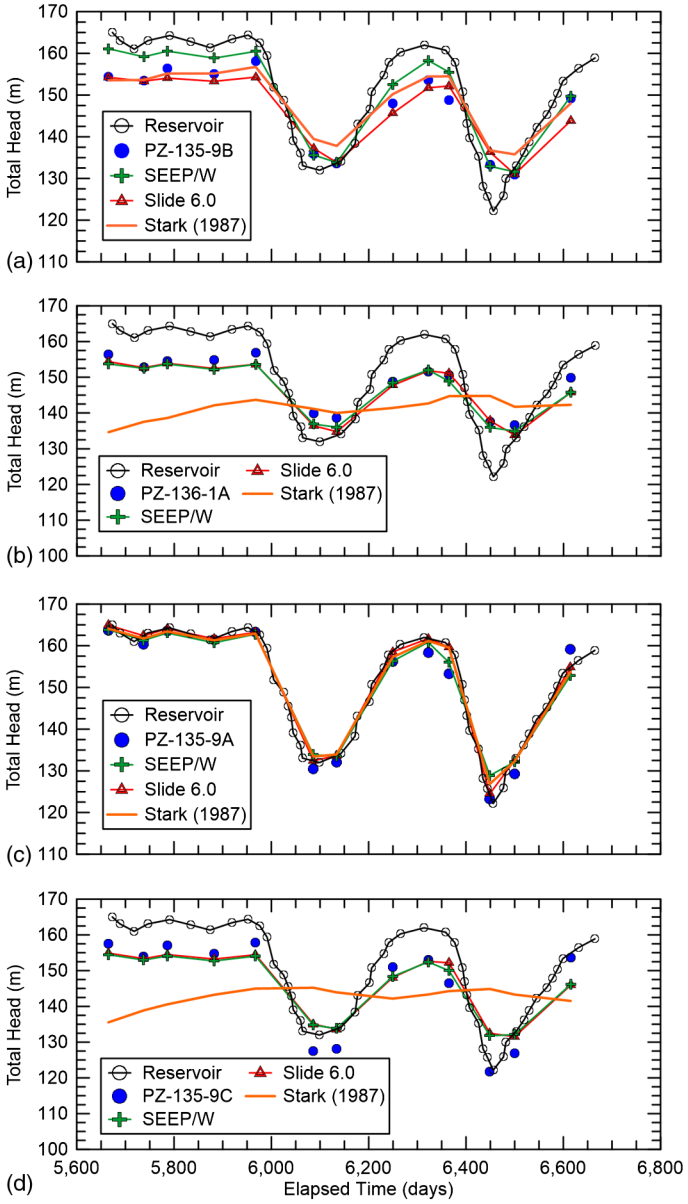

Fig. 7. Total head response in (a) slopewash; (b) Zone 1; (c) Zone 3; (d) bedrock foundation during piezometer monitoring period

increased m_v by a factor of 50. At time of reservoir capacity (5,650 to 5,950 days), *SEEP/W* and *SLIDE* are in agreement but over predict the measured total heads. During drawdown (5,950 to 6,150 and 6,350 to 6,500 days), the predicted responses in both software suggest they are in agreement with measured total heads. In subsequent refilling (6,150 to 6,350 days), *SLIDE* and *SEEP/W* again slightly overpredict the measured total heads. At the end of the analysis, the predicted total head from both programs is approximately the observed response in the field. In summary, the calibrated slopewash parameters produce good agreement with field measurements during drawdown, which is key for analysis of the 1981 slide and refilling.

Because the Zone 1 fine-grained core remains unsaturated during the piezometer monitoring period, the unsaturated soil properties influence calibration of the Zone 1 material. By adjusting α and n parameters and saturated k_h in the van Genuchten (1980) model, agreement is obtained between the calculated and measured total heads. Variations in saturated k_h affect the total head magnitude, similar to the slopewash and Zone 3 calibration. To replicate the piezometer response, saturated k_h was increased 30 times more than the Stark (1987) value to match minimum and maximum total heads. In addition, m_v was increased by a factor of seven to capture the cyclic piezometer response. Fig. 7(b) shows the final calibrated results compared to the field observations for PZ-136-1A in Zone 1. The *SEEP/W* model consistently produced lower results than *SLIDE*, but both programs, with the exception of a small period between 6,300 and 6,350 days, slightly underpredict the total head in Zone 1. The largest variance between field and calculated total heads occurs during periods of drawdown, which may be attributed to using one HCF for both the wetting and drying SWRCs.

Zone 3 operates under the same saturated seepage mechanism as the slopewash, i.e., saturated k_h, k_h/k_v, and m_v, so adjusting these parameters yields similar results. Unlike the slopewash response, adjusting the foundation k_h resulted in a smaller influence on Zone 3 because the slopewash underlies the Zone 3 and acts as a buffer for changes in the foundation. PZ-135-9A follows the fluctuations of reservoir levels, and the final calibration results for Zone 3 are shown in Fig. 7(c). *SLIDE* and *SEEP/W* produce matching total heads except from elapsed time of 5,650 to 5,950 days. During this period, *SLIDE* slightly overpredicts the total head while *SEEP/W* is approximately equal to the field results. After 5,950 days, the reservoir level decreases and *SLIDE* and *SEEP/W* slightly overpredict the total head in Zone 3. *SEEP/W* typically produces higher results than the *SLIDE* model, especially at a drawdown of 6,450 days. Difficulty in calibrating Zone 3 was attributed to less certainty in material parameters as opposed to the slopewash and Zone 1, which were tested (Von Thun 1985; Stark 1987). However, the calibrated Zone 3 parameters duplicate the field measurements during drawdown and refilling.

Fig. 7(d) compares the field (PZ-135-9C) and calculated total heads for the foundation. As indicated in Fig. 7(d), *SEEP/W* and *SLIDE* overpredict the total head during drawdown, but underpredict during filling and constant reservoir capacity. These inconsistencies could be attributed to the inability to model a nonhomogenous material like the sheared and fractured foundation bedrock.

The process of replicating piezometer readings and the interaction of soil layers resulted in the engineering properties shown in Table 3. Zone 1, Zone 3, and slopewash are assumed to be equal to k_h/k_v ratios of 2 while a value of unity (1.0) is assumed for the foundation. In addition, the compatibility of m_v and saturated k_h for the slopewash and Zone 1 materials was verified with recommendations in Stark et al. (2014). Table 3 also summarizes the changes from the original values of Stark (1987) with variations depending on the material. For the slopewash to match field results, saturated k_h was decreased from the Stark (1987) value to reduce the total head magnitude. An increase in m_v was also required to compensate for the adjustment of saturated k_h and to replicate the pore-water pressure response compared to field data. Changes in the slopewash m_v value shows more sensitivity than saturated k_h. For Zone 1, raising the saturated k_h and m_v from the Stark (1987) values was required to achieve good agreement with field data. In the case of Zone 1, pore-water pressure response is more sensitive to saturated k_h than to m_v because adjustments to saturated k_h changes the shape and location of the phreatic surface. Thus, the progression of phreatic surface has a great impact in the response of the unsaturated Zone 1 material.

A sensitivity analysis of slopewash parameters (m_v, k_h, and k_h/k_v) was performed to determine the uniqueness of the inverse analysis. Supplemental Fig. S1 shows the difference between *SLIDE* predicted values and measured total heads, i.e., Difference (P-M). For each parameter, the calibrated value was varied until the

Table 3. Summary of Calibrated Seepage Properties and Changes from Initial Properties

Material	k_h (cm/s)	k_h/k_v	m_V (kPa^{-1})	θ_S	θ_R	$1/\alpha$ (m)	n
Zone 1	1×10^{-5} (30× ↑)	2	8.35×10^{-6} (N/A)	0.29	0.05	4.2	4.5
Zone 3	1.5×10^{-6} (1.1× ↑)	2	1.0×10^{-6} (3.3× ↓)	0.27	0.02	28.6	3.2
Slopewash	1.0×10^{-8} (4.2× ↓)	2	3.5×10^{-6} (6.5× ↓)	0.24	0.02	50	2.6
Foundation	1.4×10^{-4} (37× ↑)	1	1.67×10^{-5} (N/A)	—	—	—	—

pore-water pressure response deviated significantly from the calibrated response. For example, varying m_v by an order of magnitude in Fig. S1(b) indicates limited change from the calibrated value of 3.5×10^{-6} kPa^{-1}. When 3.5×10^{-4} and 3.5×10^{-8} kPa^{-1} were selected, the predicted total head diverged from the calibrated parameter. Thus, Fig. S1(b) suggests that a broad range of m_v values from 1×10^{-5} to 1×10^{-7} kPa^{-1} can capture the time-dependent total head response in the slopewash. For saturated k_h, the calibrated value of 1×10^{-8} cm/s overpredicts the measure pore-water pressures. However, it manages to accurately capture the drawdown total head response, as indicated by data points at 6,080 days and 6,450 days in Fig. S1(c). The drawdown sequence is the most important segment of the calibration period because these pore-water pressures will be incorporated in stability analyses. In contrast, k_h of 1×10^{-7} and 1×10^{-6} cm/s trends underpredict the drawdown total heads, even though they are closer in agreement with the measured piezometer readings. The sensitivity analysis for k_h/k_v in Fig. S1(d) suggests that a $k_h/k_v > 1$ is sufficient to capture the time-dependent total head response in the slopewash. In summary, the slopewash sensitivity analyses indicate that a range of values may be appropriate for m_v and k_h/k_v, given these parameters are defined within the appropriate soil type and material property range. A unique solution exists for saturated k_h because the magnitude of pore-water pressure change is controlled by k_h, whereas m_v dictates the time lag in pore-pressure response from changing reservoir levels.

Sensitivity of Van Genuchten Parameters

The unsaturated parameters α and n in the van Genuchten (1980) model represented a significant role in the calibration process and should be emphasized in other unsaturated and transient seepage analyses. The van Genuchten (1980) parameters influence the shape and position of the SWRC and HCF graphs (Fig. 1). Zone 1 calibration relied on PZ-136-1A because no response was measured at PZ-135-10A, indicating that this portion of the fined-grained core remained unsaturated during the monitoring period. Because of the importance of the van Genuchten (1980) parameters in the calibration process, a parametric analysis of Zone 1 is provided to demonstrate the influence of α and n (Fig. 8). Fig. 8(a) presents the reservoir hydrograph and piezometer response while Figs. 8(b and c) show the computed results using *SLIDE* when α ranges from 0.05 to 2 m^{-1} at $n = 4.5$ and when n ranges from 1.5 to 4.5 with $\alpha = 0.24$ m^{-1}, respectively. The SWRC and HCF for each case is shown in Fig. 1. Figs. 8(b and c) show that varying α has a greater influence than the parameter n on the difference between *SLIDE* predicted values and measured total heads, i.e., Difference (P-M). In particular, the closest agreement to the piezometer readings for α approaches a specific value of 0.24 m^{-1} [Fig. 8(b)]. In contrast, Fig. 8(c) suggests that a unique value of n is not determined because the trend lines converge together. This outcome can be explained by Fig. 1(c), which shows that the HCF does not significantly vary for the range of n values. In summary, the Zone 1 sensitivity analyses found a unique solution for α while a range of n values are acceptable to reproduce the field behavior.

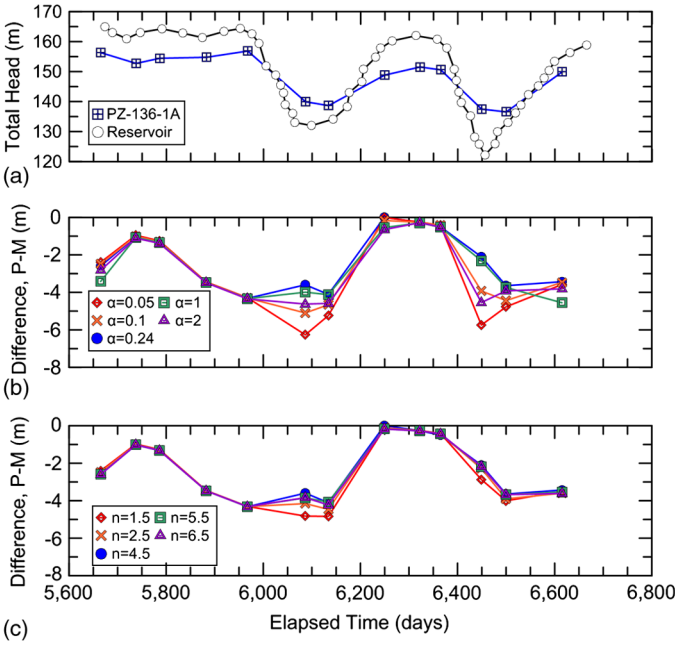

Fig. 8. Sensitivity analyses of van Genuchten (1980) parameters α and n: (a) reservoir levels and piezometer data; (b) effect of α; (c) effect of n

Based on the parametric analysis, the first effect of parameters α and n is during periods of changing reservoir level, i.e., drawdown and filling. The largest discrepancy between predicted total head and observed piezometer measurements are found at elapsed time periods of 6,000 to 6,150 days and from approximately 6,350 to 6,650 days. Both time periods correspond to periods of drawdown and subsequent filling [see reservoir level in Fig. 8(a)]. During constant reservoir levels, the SWRC and HCF corresponding to different α and n parameters provide nearly identical results.

The parameter α is related to the volumetric water content at which air first begins to enter the largest soil pores. As α decreases, the air entry condition also lowers so desaturation begins at lower matric suction. In the present study, α value of 0.24 m^{-1} results in the best fit to the field measurements. For values of α greater than 0.24 m^{-1} (1 or 2 m^{-1} in the parametric study), the difference in predicted and measured total heads, i.e., Difference (P-M), in Fig. 8(b) is more pronounced because a value of $\alpha = 0.24$ m^{-1} results in an equal or larger hydraulic conductivity at a specific matric suction compared to $\alpha = 1$ or 2 m^{-1}. This decrease in hydraulic conductivity for $\alpha = 1$ or 2 m^{-1} prevents drainage at times of reservoir drawdown and contributes to the lag experienced when the reservoir begins to fill following drawdown.

The parameter n corresponds to the pore size distribution of the material and is related to the S-shaped curvature in the SWRC and HCF. As shown in Fig. 1(c), n values lower than the calibrated value of 4.5 affect the SWRC and HCF more than n values of 5.5 or 6.5 by decreasing the slope between saturated and residual volumetric moisture contents. As a result, Fig. 8(c) shows the values of n at 1.5 and 2.5 create the largest difference between predicted and

observed, and n values of 5.5 and 6.5 produce nearly identical total head values as the calibrated van Genuchten (1980) parameters in Table 3 ($\alpha^{-1} = 4.2$ m, $n = 4.5$).

Slopewash Pore-Water Pressures

The 1981 upstream failure surface passed through the slopewash at a depth of 3 to 15 m (Stark 1987), so evaluating the pore-water pressures at failure in the slopewash is necessary to perform inverse stability analyses. The main objective is to compare the slopewash pore-water pressures from *SEEP/W* and *SLIDE* with Stark (1987). Pore-water pressures are reported herein at the middle and top of slopewash to provide an upper and lower bound, respectively, for the stability analyses. The pressure-heads at the top of slopewash in Fig. 9(a) are depicted along the horizontal length of slopewash from the slope toe to Zone 1. As discussed in the "Parent Analysis" and "Calibrated Soil Properties" sections, when the same geometry, boundary conditions, material properties, and meshing are applied, *SEEP/W* and *SLIDE* yield similar results. Maximum pore-water pressures occur near the middle of the slopewash (horizontal distance $= -145$ m and decrease in both directions for Stark (1987), *SEEP/W*, and *SLIDE*. Stark (1987) and *SEEP/W* and *SLIDE* pressure heads are about 18 and 14 m at this location, respectively, and are in good visual agreement. Variations between Stark (1987) and this study are attributed to the value of foundation saturated k_h. Stark (1987) models the foundation as an impermeable material, whereas this study uses a saturated k_h of 1.3×10^{-4} cm/s. As a result, pore-water pressures in Stark (1987) are higher, especially in the first half of the slopewash (horizontal distance from -210 to -145 m).

Fig. 9(b) shows a comparison of pressure head for the middle of slopewash for Stark (1987) and this study. The present analyses do not capture the peak pressure head of 42 m exhibited at horizontal distance of -83 m from Stark (1987). The *SEEP/W* and *SLIDE* results indicate a maximum pressure head of ~21 m at a horizontal distance of -150 m. The peak pressure head of 42 m in Stark (1987) occurs at a horizontal distance of -80 m, where the Zone 1 material overlies the slopewash. These soil layers were modeled with much lower k_h values (about 2 orders of magnitude) than this study, which is important because this portion of the slopewash lies between Zone 1 and bedrock foundation (Fig. 2). Because the pore-water pressures could not drain in the vertical direction into Zone 1 or the bedrock, the high pore-water pressures in Stark (1987) are attributed to the long drainage path in the horizontal direction along the slopewash.

Phreatic Surface

Another objective of the unsaturated and transient seepage analyses is to determine the progression of the phreatic surface through the Zone 1 fine-grained core, establish when steady-state conditions are achieved in the embankment, and evaluate the phreatic surface at the time of failure. To achieve this objective, seepage through the core is analyzed using *SEEP/W* and *SLIDE* with the calibrated soil properties shown in Table 3 and the boundary conditions in Fig. 6. The phreatic surface migration through the embankment at certain time periods of San Luis Reservoir operation is shown in Fig. 10.

Fig. 10(a) shows the phreatic surface advancing through the Zone 1 core a year after San Luis Reservoir began operating. In particular, Fig. 10(a) suggests Zone 1 is saturating from water percolating through Zones 4 and 5 rockfill and via foundation underseepage. *SEEP/W* and *SLIDE* show the slopewash and Zone 3 materials saturate within the first year while Stark (1987) reports both materials remain unsaturated near the intersection of Zone 1 and foundation, which is likely due to the low saturated k_h of Zone 1 and foundation. After 1.5 years of operation [Fig. 10(b)], the slopewash and Zone 3 materials are saturated in Stark (1987), *SEEP/W*, and *SLIDE* analyses. Similar to Fig. 10(a), *SEEP/W* and *SLIDE* show the phreatic surface has progressed further into the Zone 1 core than Stark (1987), which is now showing Zone 1 saturating from both reservoir seepage and foundation underseepage. Fig. 10(c) displays the phreatic surfaces after 4.5 years with *SEEP/W* and *SLIDE* yielding a phreatic surface that is saturating the downstream Zone 4 rockfill. In contrast, Stark (1987) shows the phreatic surface still progressing through the center of Zone 1 after 4.5 years. *SEEP/W* and *SLIDE* produce phreatic surfaces that are comparable and indicate that the fine-grained core is close to steady-state conditions after 4.5 years instead of 7.5 years as indicated by Stark (1987). The phreatic surfaces after 7.5 years from Stark (1987), *SEEP/W*, and *SLIDE* are comparable in Fig. 10(d). The *SEEP/W* and *SLIDE* analyses show minor changes in the phreatic surface between 4.5 to 7.5 years while Stark (1987) analysis shows a continued progression through the center of the Zone 1 core. The inconsistent phreatic surfaces between this study and Stark (1987) are likely attributed to Stark (1987) modeling the foundation as impermeable and the different HCF relationships.

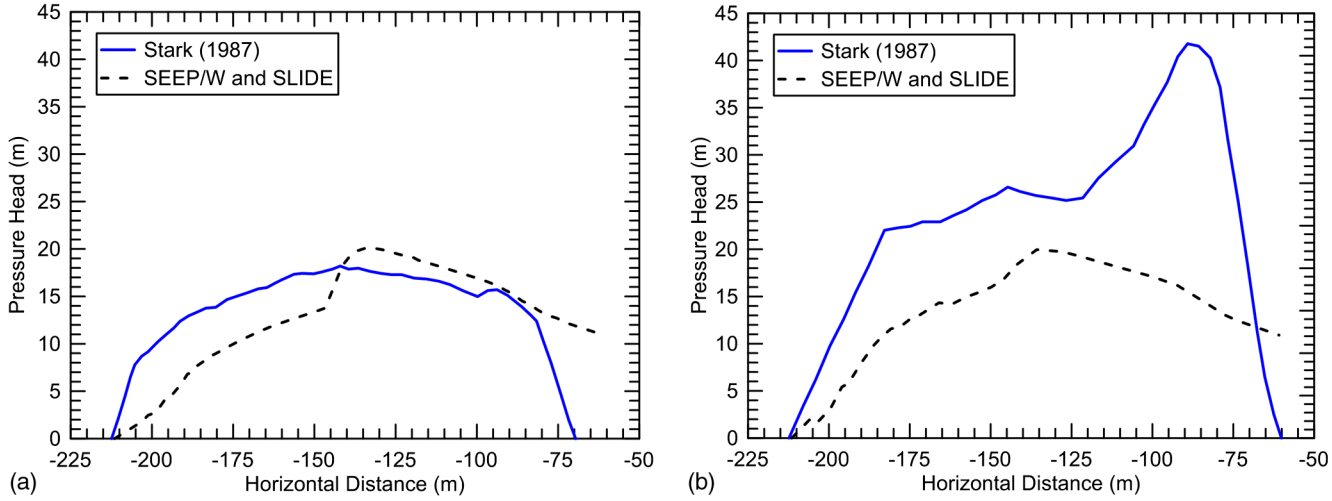

Fig. 9. Calculated seepage pressure head at the time of 1981 slide along (a) top; (b) middle of slopewash

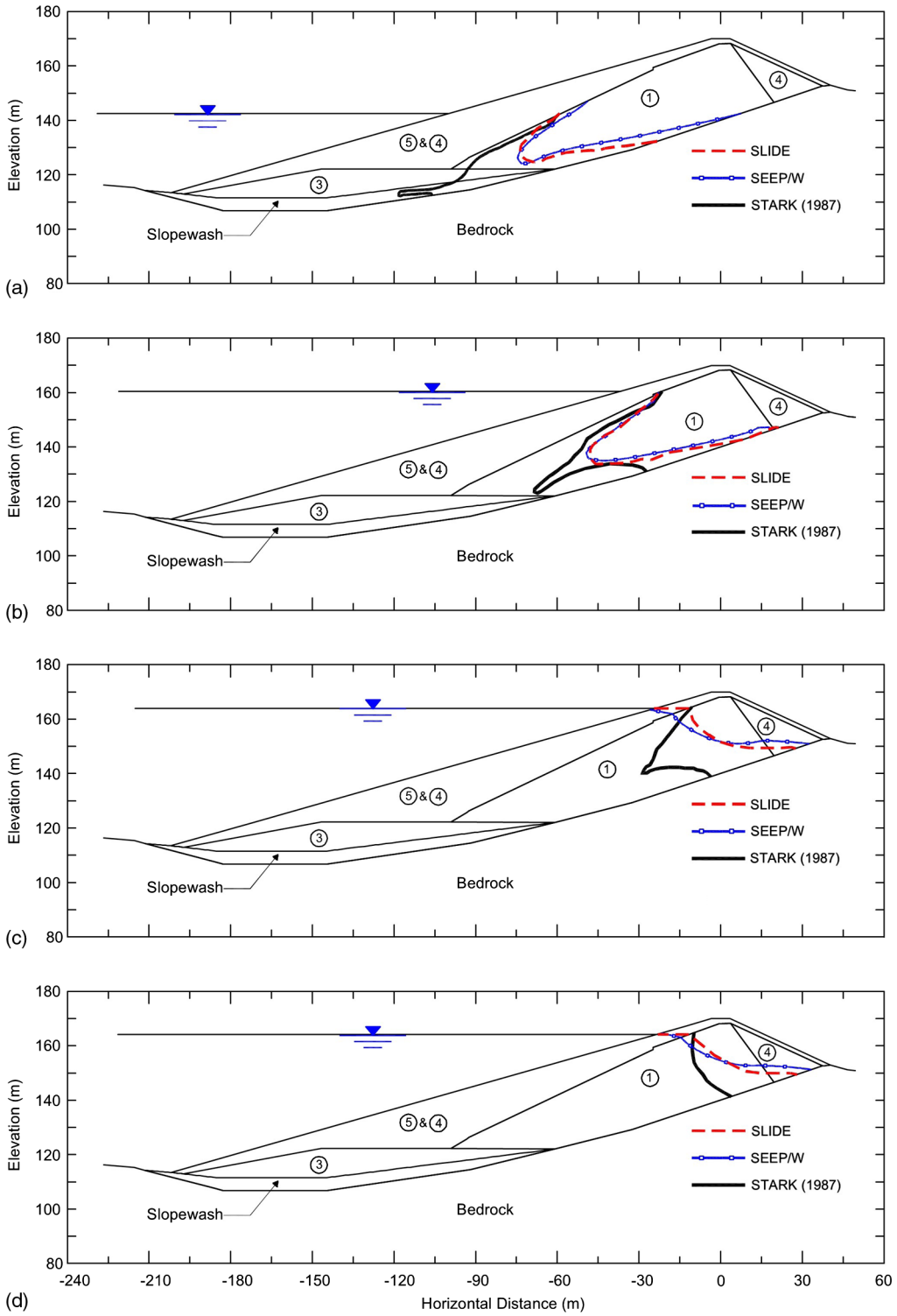

Fig. 10. Phreatic surface after (a) time = 1.0 years; (b) time = 1.5 years; (c) time = 4.5 years; (d) time = 7.5 years of reservoir operation

Still, the phreatic surface progresses in a similar manner in all three analyses, and the models indicate Zone 1 approaches steady-state conditions after about 7.5 years of reservoir operation.

Stability Analyses

A major impetus for using San Luis Dam is to investigate the decrease in factor of safety (FS) from transient seepage and shear-induced pore-water pressures because the FS should be about unity in 1981. *SLIDE* was used to compute the upstream slope FS during drawdown conditions and also analyze the prior stability analysis by Stark and Duncan (1991). The slopewash shear strength parameters obtained from direct shear and triaxial compression tests (Stark and Duncan 1991) and the resulting FS are shown in Table 4. The peak shear strengths for Zones 1 and 3 were $c' = 5.3$ kPa, $\phi' = 25°$ and $c' = 4.8$ kPa, $\phi' = 25°$, respectively (Stark and Duncan 1991).

Table 4. Calculated Factors of Safety for Upstream Slope of San Luis Dam

Condition	Stark and Duncan (1991)	Stark and Duncan (1991) using *SLIDE*		Present study	
	Failure surface 1	Failure surface 1	Failure surface 2	Failure surface 1	Failure surface 2
End of construction					
Desiccated slopewash: $c' = 263$ kPa, $\phi' = 39°$	4.0	3.9	4.8	3.7	4.7
Reservoir full					
Fully softened slopewash: $c' = 0$ kPa, $\phi' = 25°$	2.0	2.1	2.0	2.1	1.9
Reservoir drawdown					
Fully softened slopewash: $c' = 0$ kPa, $\phi' = 25°$	1.3	1.3	1.27	1.6	1.5
Reservoir drawdown					
Reduced fully softened slopewash: $c' = 0$ kPa, $\phi' = 20°$	N/A	1.2	1.08	1.45	1.25
Reservoir drawdown					
Residual slopewash: $c' = 0$ kPa, $\phi' = 15°$	1.0	1.08	0.9	1.3	1.05

To perform a stability analysis in *SLIDE*, the pore-water pressures determined at the time of failure (September 4, 1981) are exported at nodes in the transient seepage model and then imported in the slope stability analysis as a grid (Fig. 11 phreatic surface). In particular, the slopewash pore-water pressures applied in Stark and Duncan (1991) and this study are provided in Fig. 9. Stark and Duncan (1991) and *SLIDE* analyses were performed using the Spencer (1967) stability method, which satisfies all conditions of equilibrium. The Stark and Duncan (1991) failure surface (see Failure Surface 1 in Fig. 11) passes through Zone 3 based on slope inclinometer measurements projected from another station to Station 135 + 00. The hill incorporated in the dam is undulating, thus the failure surface likely extends only through the weaker slopewash at Station 135 + 00 (Fig. 11 and Failure Surface 2). Because of this uncertainty, both failure surfaces are investigated herein.

Table 4 summarizes the changes in FS for varying reservoir levels and slopewash shear strength parameters and provides a comparison of FS between this study and Stark and Duncan (1991). In particular, the first column, Stark and Duncan (1991), in Table 4 lists the FS for Failure Surface 1 as reported in Stark and Duncan (1991). The purpose of the second column, Stark and Duncan (1991) using *SLIDE*, is to reproduce the FS in the first column in *SLIDE* by using the pore-water pressures from Stark and Duncan (1991) and Failure Surface 1. The FS values under Failure Surface 2 again incorporate Stark and Duncan (1991) pore-water pressures into *SLIDE*. The third column, Present Study, presents the FS values for both failure surfaces but with updated pore-water pressures developed from this study. At the end of construction with the slopewash still highly desiccated, both analyses report FS of approximately four. During reservoir-full conditions, all analyses report FS of approximately two with the slopewash shear strength reduced to the fully softened value (Gamez and Stark 2014). When the reservoir level is lowered and the slopewash is still assigned a fully softened shear strength, Stark and Duncan (1991) report the FS decreases to 1.3 while the present study computes a FS of 1.5 for Failure Surface 2. The higher FS in this study is attributed to a lower phreatic surface in Zone 1 [Fig. 7(c) comparison of Stark (1987) and this study model results] and lower pore-water pressures in the slopewash due to the bedrock being impermeable in Stark and Duncan (1991) (see also Fig. 9). The FS for Failure Surface 2 approaches unity (1.0) for both analyses once the slopewash is reduced to residual strength. Using the pore-water pressures reported in Stark (1987) and Failure Surface 2, *SLIDE* produced a FS of 0.9. A FS at or below unity is reasonable because the seepage pore-water pressures in the slopewash (Fig. 9) are greater than the shear-induced pore-water pressures along most of the failure surface. The values of shear-induced pore-water pressures are calculated below, but on average the seepage and shear-induced pore-water pressures contribute about 65 and 35%, respectively, between the toe and downstream extent of the slopewash.

Because the slopewash is a colluvial material and subjected to cyclic shear stresses imposed by reservoir drawdowns, the shear strength can range from fully softened to residual (reduced fully softened strength in Table 4) as suggested by Stark and Eid (1997) and Stark and Duncan (1991), respectively. Therefore, an additional reservoir drawdown analysis was performed with the slopewash strength at $\phi' = 20°$, which is between the fully softened and residual friction angles. The FS is 1.45 and 1.25 for Failure Surfaces 1 and 2, respectively.

The FS values reported in Table 4 for Stark and Duncan (1991) and Failure Surface 1 are slightly greater than unity for the residual strength condition (slopewash $\phi' = 15°$), which is acceptable

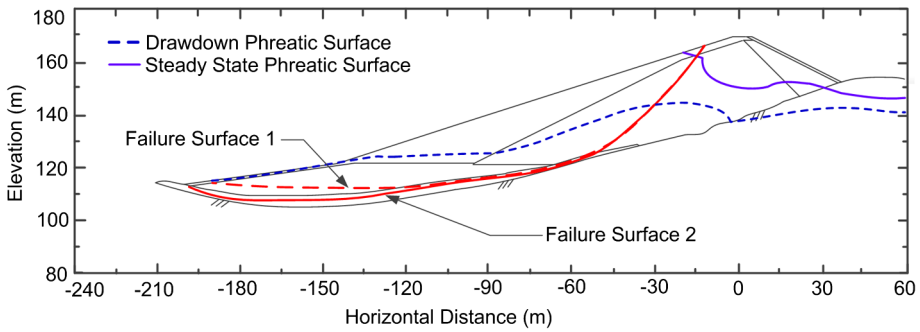

Fig. 11. Estimated upstream slide planes at station 135 + 00

because shear-induced pore-water pressures are not calculated in the transient seepage analysis and subsequently not included in the stability analysis. The effects of seepage and shear-induced pore-water pressures was inferred from the FS values at the reservoir full and drawdown conditions using only Failure Surface 2. When the stability was evaluated for only total head seepage pressures and a slopewash strength of $\phi' = 20°$, the FS value decreased from 1.45 to 1.25 after reservoir drawdown. Therefore, the FS should approach unity when shear-induced pore-water pressures are accounted for in the stability analysis. In other words, FS should decrease by about 0.25 if shear-induced pore-water pressures are included. To confirm this decrease in FS of about 0.25, the shear-induced pore-water pressures in the slopewash were estimated using Skempton's (1954) A coefficient and the change in normal total stresses along the observed failure surface due to reservoir drawdown. The A coefficient is used and not $\bar{B}$ (Bishop 1954) because only changes due to shear or deviator stresses are being considered. The value of A was calculated for the failure condition in triaxial compression tests, resulting in values of A at failure (A_f). An average A_f value of 0.42 was estimated for the slopewash using results from isotropically consolidated-undrained triaxial compression tests, with pore-water pressure measurements conducted by Stark (1987) on an upstream slopewash sample wetted by the reservoir. These triaxial compression tests show A_f ranges from 0.4 to 0.43 for effective confining pressures of 89.5 to 275.8 kPa. A value of A_f of about 0.42 is also in agreement with lightly overconsolidated clays ($A_f = 0$ to 0.5) and normally consolidated clays ($A_f = 0.5$ to 1.0) according to Skempton (1954). Because the triaxial compression tests performed by Stark (1987) at low normal stresses show the upstream slopewash is slightly overconsolidated even after reservoir filling, a value of A_f close to 0.5 is reasonable.

The shear-induced pore-water pressures along the slopewash failure surface was estimated using A_f of 0.42 and the change in normal total stress caused by lowering of the reservoir. The transient seepage pore-water pressures from *SLIDE* and shear-induced pore-water pressures estimated from the A_f value were combined together to estimate the total pore-water pressure acting on each slice along the failure surface. The normal effective stresses on each slice were estimated from the normal total stress obtained from *SLIDE* and estimated total pore-water pressure, which were then used to determine the mobilized shear strength along the failure surface. The resulting FS is 1.02, which suggests the transient seepage and shear-induced pore-water pressures can be separately evaluated and combined to provide a reasonable value of FS for this case history. Although coupled hydro-mechanical analyses are more complex than transient seepage analyses, they are recommended to directly account for the interactions of transient flow, shear-induced volume change, and consolidation due to changes in reservoir levels (Alonso and Pinyol 2011).

Summary

This paper uses a piezometer calibrated seepage model of San Luis Dam to illustrate the influence and effect of rapid drawdown on the upstream slope. The unsaturated and transient seepage analysis utilized two available software packages (*SEEP/W* and *SLIDE*) to predict the migration of phreatic surface during various reservoir levels and evaluate the influence of unsaturated properties on pore-water pressure dissipation during drawdown. The following information and recommendations were derived from the analyses:

- The van Genuchten (1980) unsaturated soil model uses α and n parameters to model the SWRC and HCF. Increasing α shifts the SWRC and HCF to lower matric suction without changing the overall shape of the curve while the parameter n steepens the SWRC and HCF slope between θ_s and θ_r. Adjusting these parameters in the parametric study shows that α causes a greater impact on pore-water pressure response than n. In particular, increasing α lowers the HCF and inhibits pore-water pressure from draining at time of drawdown, which contributes to the lag time experienced in subsequent refilling. Therefore, practitioners should place significant emphasis on estimating α, which corresponds to the air entry value in the SWRC.
- Initial suction conditions for an unsaturated and transient seepage analysis can be estimated using a steady-state analysis. For *SEEP/W* and *SLIDE* to yield comparable steady-state results and initial suctions, the following input and model parameters must be similar: unsaturated properties and functions, dam geometry, boundary conditions, material properties, and meshing technique. The steady-state results serve as the start or origin of the transient seepage analysis. In practice, in situ measurement of volumetric moisture content and suction should be utilized to validate the calculated initial suction profile.
- Unsaturated and transient seepage analyses can be used to estimate the pore-water pressures caused by changes in hydraulic conditions for input in an ESSA with shear-induced pore-water pressures that are estimated using A_f. For example, *SEEP/W* and *SLIDE* predicted the seepage-induced pore-water pressures at the time of the 1981 slide. As a result, this case history suggests slope stability analyses can be performed for a range of drawdown rates without requiring undrained shear strengths at multiple consolidation pressures and conditions.

Acknowledgments

The contents and views in this paper are those of the authors and do not necessarily reflect those of any dam or reservoir owner/operator, consultant, regulatory agency or personnel, or anyone else knowledgeable about the case study referenced. In particular, the contents of this paper/publication are the personal opinions of the author(s) and may not reflect the opinions, conclusions, policies or procedures of the U.S. Bureau of Reclamation or U.S. Army Corps of Engineers.

Supplemental Data

Fig. S1 is available online in the ASCE Library (www.ascelibrary.org).

References

Alonso, E., and Pinyol, N. (2009). "Slope stability under rapid drawdown conditions." *Rainfall-induced landslides: Mechanisms, monitoring techniques, and nowcasting models for early warning systems*, L. Picarelli, P. Tommasi, G. Urciuoli, and P. Versace, Naples, Italy, 11–27.

Alonso, E. E., and Pinyol, N. M. (2011). "Landslides in reservoirs and dam operation." *Dam maintenance and rehabilitation II*, R. Garcia, et al., eds., CRC Press, 3–27.

Baker, R., Frydman, S., and Talesnick, M. (1993). "Slope stability analysis for undrained loading conditions." *Int. J. Numer. Anal. Methods Geomech.*, 17(1), 15–43.

Bareither, C. A., and Bension, C. H. (2013). "Evaluation of Bouwer-Rice large-particle correction procedure for soil water characteristic curves." *Geotech. Test. J.*, 36(5), 1–15.

Benson, C., Chiang, I., Chalermyanont, T., and Sawangsuriya, A. (2014). "Estimating van Genuchten parameters α and n for clean sands from particle size distribution data." *Soil Behavior Fundamentals to*

Innovations in Geotechnical Engineering, Geo-Congress 2014, ASCE, Reston, VA, 410–427.
Berilgen, M. (2007). "Investigation of stability of slopes under drawdown conditions." *Comput. Geotech.*, 34(2), 81–91.
Bishop, A. W. (1952). "The stability of earth dams." Ph.D. thesis, Univ. of London, London.
Bishop, A. W. (1954). "The use of pore-water coefficients in practice." *Geotechnique*, 4(4), 148–152.
Bishop, A. W., and Bjerrum, L. (1960). "The relevance of the triaxial test to the solution of stability problems." *Proc., Research Conf. on the Shear Strength of Cohesive Soils*, ASCE, Reston, VA, 437–501.
Brooks, R. H., and Corey, A. T. (1964). "Hydraulic properties of porous media." Colorado State Univ., Fort Collins, CO.
Burdine, N. T. (1953). "Relative permeability calculations from pore size distribution data." *Petr. Trans. AIME*, 198, 71–78.
Casagli, N., Rinaldi, M., Gargini, A., and Curini, A. (1999). "Pore water pressure and streambank stability: Results from a monitoring site on the Sieve River, Italy." *Earth Surf. Processes Landforms*, 24(12), 1095–1114.
Casagrande, A. (1937). "Seepage through dams." *J. New England Water Works Assoc.*, 51(2), 131–172.
Casagrande, A. (1961). "Control of seepage through foundations and abutments of dams." *Geotechnique*, 11(3), 161–182.
Cooley, R. L. (1983). "Some new procedures for numerical solution of variably saturated flow problems." *Water Resour. Res.*, 19(5), 1271–1285.
Desai, C. S. (1972). "Seepage analysis of earth banks under drawdown." *J. Soil Mech. Found. Div.*, 98(11), 1143–1162.
Desai, C. S. (1977). "Drawdown analysis of slopes by numerical method." *J. Geotech. Geoenviron. Eng.*, 103(7), 667–676.
Desai, C. S., and Sherman, W. C. (1971). "Unconfined transient seepage in sloping banks." *J. Soil Mech. Found. Div.*, 97(2), 357–373.
Duncan, J. M., Wright, S. G., and Wong, K. S. (1990). "Slope stability during rapid drawdown." *Proc., H. Bolten Seed Memorial Symp.*, Vol. 2, BiTech, Vancouver, BC, Canada.
Fredlund, D. G., and Rahardjo, H. (1993). *Soil mechanics for unsaturated soils*, Wiley, New York.
Fredlund, D. G., and Xing, A. (1994). "Predicting the permeability functions for unsaturated soils using the soil water characteristic curve." *Can. Geotech. J.*, 31(4), 533–546.
Freeze, R. A., and Cherry, J. A. (1979). *Groundwater*, Prentice-Hall, Englewood Cliffs, NJ.
Gamez, J., and Stark, T. D. (2014). "Fully softened shear strength at low stresses for levee and embankment design." *J. Geotech. Geoenviron. Eng.*, 10.1061/(ASCE)GT.1943-5606.0001151, 06014010-1–06014010-6.
ICOLD (International Committee on Large Dams). (1980). *Deterioration of dams and reservoirs. Examples and their analyses*, Balkema, Rotterdam, Netherlands.
Jones, F. O., Embody, D. R., and Peterson, W. L. (1961). "Landslides along the Columbia River Valley, Northeastern Washington." U.S. Geological Survey Professional Paper, Washington, DC.
Lam, L., Fredlund, D. G., and Barbour, S. L. (1987). "Transient seepage model for saturated-unsaturated systems: A geotechnical engineering approach." *Can. Geotech. J.*, 24(4), 565–580.
Lambe, T. W., and Whitman, R. V. (1969). *Soil mechanics*, Wiley, NY.
Lane, K. S. (1967). "Stability of reservoir slopes." *Proc., 8th Symp. on Rock Mechanics*, Univ. of Minnesota, Minneapolis, 321–336.
Lane, P., and Griffiths, D. (2000). "Assessment of stability of slopes under drawdown conditions." *J. Geotech. Geoenviron. Eng.*, 10.1061/(ASCE)1090-0241(2000)126:5(443), 443–450.
Lowe, J., and Karafiath, L. (1959). "Stability on earth dams upon drawdown." *Proc., Pan-American Conf. on Soil Mechanics and Foundation Engineering*, Mexican Society of Soil Mechanics, Mexico, DF, 537–552.
Lowe, J., and Karafiath, L. (1960). "Effect of anisotropic consolidation on the undrained shear strength of compacted clays." *Proc., Research Conf. on Shear Strength of Cohesive Soils*, 837–858.
Lu, N., and Likos, W. J. (2004). *Unsaturated soil mechanics*, Wiley, New York.
Mansur, C. I., Kaufman, R. I., and Schultz, J. R. (1956). "Investigation of underseepage and its control, lower Mississippi River levees." *Technical Memorandum No. TM 3-424*, USACE Waterways Experiment Station, U.S. Army Corps of Engineers, Vicksburg, MI.
Mansur, C. I., Postol, G., and Salley, J. R. (2000). "Performance of relief well systems along Mississippi River levees." *J. Geotech. Geoenviron. Eng.*, 10.1061/(ASCE)1090-0241(2000)126:8(727), 727–738.
Morgenstern, N. R. (1963). "Stability charts for earth slopes during rapid drawdown." *Geotechnique*, 13(2), 121–131.
Mualem, Y. (1976). "A new model for predicting the hydraulic conductivity of unsaturated porous media." *Water Resour. Res.*, 12(3), 513–522.
Neumann, S. P. (1973). "Saturated-unsaturated seepage by finite elements." *J. Hydraulic Div.*, 99, 2233–2250.
Pauls, G. J., Karlsauer, E., Christiansen, E. A., and Wigder, R. A. (1999). "A transient analysis of slope stability following drawdown after flooding of highly plastic clay." *Can. Geotech. J.*, 36(6), 1151–1171.
Pinoyl, N. M., Alonso, E. E., and Olivella, S. (2008). "Rapid drawdown in slopes and embankments." *Water Resour. Res.*, 44(5), 1–22.
Rinaldi, M., and Casagli, N. (1999). "Stability of streambanks formed in partially saturated soils and effects of negative pore water pressures: The Sieve River (Italy)." *Geomorphology*, 26(4), 253–277.
Rinaldi, M., Casagli, N., Dapporto, S., and Gargini, A. (2004). "Monitoring and modelling of pore water pressure changes and riverbank stability during flow events." *Earth Surf. Processes Landforms*, 29(2), 237–254.
SEEP/W [Computer software]. Geo-Slope International, Calgary, Canada.
Sherard, J. L. (1953). "Influence of soil properties and construction methods on the performance of homogeneous earth dams." *Tech. Memo. 645*, U.S. Bureau of Reclamation, Denver.
Sherard, J. L., Woodward, R. J., Gizienski, S. G., and Clevenger, W. A. (1963). *Earth and earth-rock dams*, Wiley, New York.
Skempton, A. (1954). "The pore-pressure coefficients A and B." *Geotechnique*, 4(4), 143–147.
SLIDE version 6.0 [Computer software]. Rocscience, Toronto.
Spencer, E. (1967). "A method of analysis of the stability of embankments assuming parallel interslice forces." *Geotechnique*, 17(1), 11–26.
Stankovich, J., and Lockington, D. (1995). "Brooks-Corey and van Genuchten soil-water-retention models." *J. Irrig. Drain. Eng.*, 10.1061/(ASCE)0733-9437(1995)121:1(1), 1–7.
Stark, T. D. (1987). "Mechanisms of strength loss in stiff clays." Ph.D. thesis, Dept. of Civil and Environmental Engineering, Virginia Polytechnic Institute and State Univ., Blacksburg, VA.
Stark, T. D., and Duncan, J. M. (1991). "Mechanisms of strength loss in stiff clays." *J. Geotech. Eng.*, 10.1061/(ASCE)0733-9410(1991)117:1(139), 139–154.
Stark, T. D., and Eid, H. T. (1997). "Slope stability analyses in stiff fissured clays." *J. Geotech. Geoenviron. Eng.*, 10.1061/(ASCE)1090-0241(1997)123:4(335), 335–343.
Stark, T. D., Jafari, N. H., Leopold, A. L., and Brandon, T. L. (2014). "Soil compressibility in transient unsaturated seepage analyses." *Can. Geotech. J.*, 51(8), 858–868.
Terzaghi, K., Peck, P. B., and Mesri, G. (1996). *Soil mechanics in engineering practice*, Wiley, New York.
Thieu, N. T. M., Fredlund, M. D., Fredlund, D. G., and Hung, V. Q. (2001). "Seepage modeling in a saturated/unsaturated soil system." *Proc., Int. Conf. on Management of the Land and Water Resources*, 1–8.
Tinjum, J., Benson, C., and Blotz, L. (1997). "Soil-water characteristic curve for compacted clays." *J. Geotech. Geoenviron. Eng.*, 10.1061/(ASCE)1090-0241(1997)123:11(1060), 1060–1069.
Turnbull, W. J., and Mansur, C. I. (1961). "Investigation of underseepage—Mississippi River levees." *Trans. ASCE*, 126, 1486–1539.
USACE. (1970). "Engineering and design slope stability." *ETL 1110-2-1902*, Dept. of the Army, Washington, DC.
USBR. (2013). "Central valley project." ⟨http://www.usbr.gov/projects/Project.jsp?proj_Name=Central+Valley+Project⟩ (Nov. 24, 2014).
Valiantzas, J. (2011). "Combined Brooks-Corey/Burdine and van Genuchten/Mualem closed-form model for improving prediction of unsaturated conductivity." *J. Irrig. Drain. Eng.*, 10.1061/(ASCE)IR.1943-4774.0000284, 223–233.
van Genuchten, M. T. (1980). "A closed-form equation for predicting the hydraulic conductivity of unsaturated soils." *Soil Sci. Soc. Am. J.*, 44(5), 892–898.
VonThun, J. L. (1985). "San Luis dam upstream slide." *Proc., 11th Int. Conf. on Soil Mechanics and Foundation Engineering*, A. A. Balkema, Rotterdam, Netherlands, 2593–2598.

Wolff, T. F. (1974). "Performance of underseepage control measures during the 1973 Mississippi River Flood: Columbia levee district, Illinois." M.Sc. thesis, Oklahoma State Univ., Stillwater, OK.
Wolff, T. F. (1989). "Levee underseepage analysis for special foundation conditions." *Research Rep. REME-GT-11*, U.S. Army Corps of Engineers Waterways Experiment Station, U.S. Army Corps of Engineers, Vicksburg, MI.
Wright, S. G., and Duncan, J. M. (1987). "An examination of slope stability computation procedures for sudden drawdown." *Miscellaneous Paper GL-87-25*, Geotechnical Laboratory, USACE, WES, Vicksburg, MI.